Journal of Virology

Immunology | Full-Length Text

Insulin-mediated endothelin signaling is antiviral during West Nile virus infection

Chasity E. Trammell,[1] Evelyn H. Rowe,[1] Aditya B. Char,[1] Brianne J. Jones,[1] Stephen Fawcett,[1] Laura R. H. Ahlers,[2] Alan G. Goodman[1,3]

AUTHOR AFFILIATIONS See affiliation list on p. 15.

ABSTRACT West Nile virus (WNV) is the most prevalent mosquito-borne virus in the United States with approximately 2,000 cases each year. There are currently no approved human vaccines and a lack of prophylactic and therapeutic treatments. Understanding host responses to infection may reveal potential intervention targets to reduce virus replication and disease progression. The use of *Drosophila melanogaster* as a model organism to understand innate immunity and host antiviral responses is well-established. Previous studies revealed that insulin-mediated signaling regulates WNV infection in invertebrates by regulating canonical antiviral pathways. Because insulin signaling is well-conserved across insect and mammalian species, we sought to determine if results using *D. melanogaster* can be extrapolated for the analysis of orthologous pathways in humans. Here, we identify insulin-mediated endothelin signaling using the *D. melanogaster* model and evaluate an orthologous pathway in human cells during WNV infection. We demonstrate that endothelin signaling reduces WNV replication through the activation of canonical antiviral signaling. Taken together, our findings show that endothelin-mediated antiviral immunity is broadly conserved across species and reduces replication of viruses that can cause severe human disease.

IMPORTANCE Arboviruses, particularly those transmitted by mosquitoes, pose a significant threat to humans and are an increasing concern because of climate change, human activity, and expanding vector-competent populations. West Nile virus is of significant concern as the most frequent mosquito-borne disease transmitted annually within the continental United States. Here, we identify a previously uncharacterized signaling pathway that impacts West Nile virus infection, namely endothelin signaling. Additionally, we demonstrate that we can successfully translate results obtained from *D. melanogaster* into the more relevant human system. Our results add to the growing field of insulin-mediated antiviral immunity and identify potential biomarkers or intervention targets to better address West Nile virus infection and severe disease.

KEYWORDS RNA sequencing, *Drosophila melanogaster*, immunity, AKT, CG43775

West Nile virus (WNV) is a member of the family *Flaviviridae* and is transmitted predominately between *Culex quinquefasciatus* and birds with humans as incidental "dead-end" hosts (1). WNV was introduced to the Western Hemisphere in New York in 1999 and has since become endemic in the United States (2–4). Like other arthropod-borne viruses, WNV poses a significant health threat due to the expansion of mosquito range and activity (5–7) without effective means to address these concerns at a transmission or clinical level. While our ability to intervene in arboviral exposure at the vector-transmission level has progressed significantly in the past decade through genetic (8), microbial (9), or small molecule (10) targeting of mosquito responses, addressing WNV clinical cases has lagged. There are currently no vaccines or specific treatments

Editor Mark T. Heise, University of North Carolina at Chapel Hill, Chapel Hill, North Carolina, USA

Address correspondence to Alan G. Goodman, alan.goodman@wsu.edu.

The authors declare no conflict of interest.

See the funding table on p. 15.

Received 24 July 2023
Accepted 20 August 2023
Published 5 October 2023

available for treating WNV with the best approaches being disease management and pain relief (11).

Drosophila melanogaster is an established model organism that has been used for studying host responses. This is due to its readily accessible and annotated genome that permits broad or targeted study of specific signaling pathways or interactions. *D. melanogaster* has been successfully used to study innate immune responses to flavivirus infection including WNV (12, 13) and Zika virus (ZIKV) (14). Previous investigation identified insulin-mediated induction of JAK/STAT as a critical component of host survival and immunity to WNV in *D. melanogaster* that was conserved in *Culex quinquefasciatus* (13). Because of the broad conservation that the insulin signaling pathway is across species, especially from *D. melanogaster* to human systems (15, 16), we rationalize that insulin-mediated antiviral immunity may exist in the human innate immune system as well. Previous studies have shown that viral infection may target components of insulin signaling that can result in insulin resistance and dysfunction (17–21), but there is limited investigation about how this host-virus interaction can be a potential intervention target. Because of the substantial number of downstream signaling pathways insulin signaling impacts, we sought to identify previously unidentified signaling pathways that canonical insulin signaling regulates and may have important roles in the host response to viral infection. In addition, because of the significant conservation that insulin signaling possesses across species and the genetic power of the *D. melanogaster* model, we propose that we can extrapolate identified pathways from *D. melanogaster* and their orthologous pathways in the human system.

In this study, we performed RNA sequencing (RNAseq) in *D. melanogaster* during WNV infection to identify novel antiviral response elements that are activated in the presence of insulin. We find that insulin induces numerous genes including canonical antiviral response elements as well as genes that were previously uncharacterized components of host immunity. We then evaluate the impact that genes identified within an enriched cluster have for host responses to WNV infection in *D. melanogaster*. We found that disruption of genes associated with this cluster increased host mortality in *D. melanogaster*. This gene cluster was associated with endothelin signaling, which is primarily associated in vasoconstriction and cardiovascular function (22) but has been suggested as a biomarker for various infectious disease pathogenesis (23–25), immune dysregulation (26, 27), and insulin sensitivity (28, 29). We then used this information to evaluate endothelin signaling in human cells. We similarly found that endothelin signaling was important for regulating viral replication and regulating insulin-mediated responses to infection against both attenuated and virulent WNV strains. These results suggest that insulin regulates endothelin signaling such that the loss of endothelin results in deficient host antiviral immunity. These pathways are conserved across species and may be a potential avenue for future therapeutic research.

RESULTS

Transcriptomic profiling of *D. melanogaster* S2 cells identifies antiviral pathways linked to insulin signaling

We first sought to generate a complete transcript profile of *D. melanogaster* S2 cells following 24-h treatment with 1.7 µM bovine insulin and 8-h infection with WNV-Kun by RNAseq. Gene expression in treated and/or infected cells was measured relative to that in controls receiving neither bovine insulin nor virus (Fig. 1A). These experimental conditions were selected based on previous data showing that bovine insulin treatment induces sufficient insulin and JAK/STAT signaling in S2 cells (13). Triplicate biological replicates were measured in duplicate and averaged (Table S1, Sheet 1). The average proportion of sequence reads mapped to the *D. melanogaster* genome was approximately 93.22% (Table S1, Sheet 1). Principal component analysis showed that biological replicates clustered together with insulin treatment being the major principal component causing 37.3% variation among samples, whereas WNV-Kun infection caused 7.2% variation (data not shown).

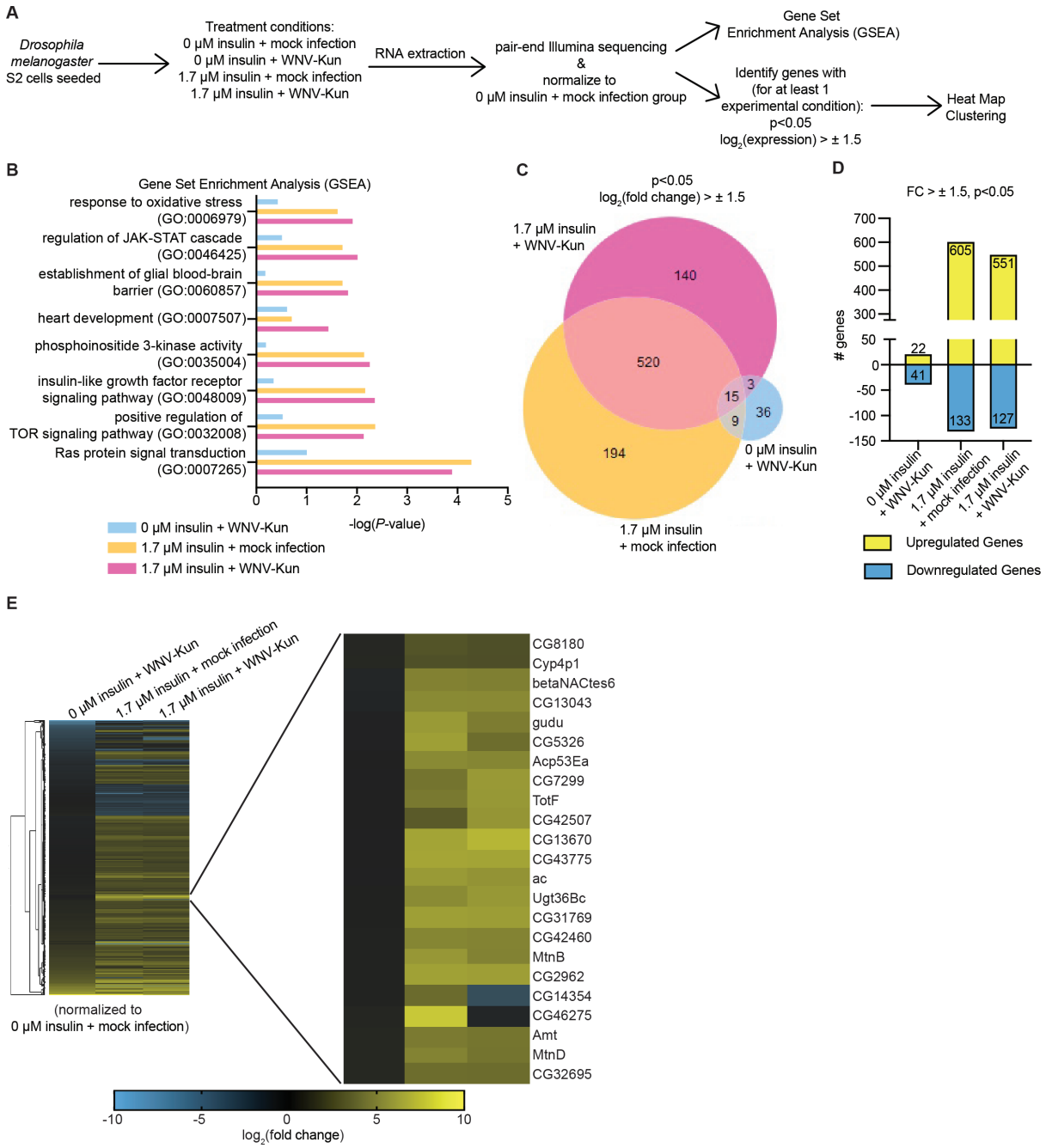

FIG 1 Insulin treatment during WNV-Kun infection in *D. melanogaster* S2 cells induces canonical and previously unidentified signaling pathways. (A) Schematic illustrating experimental design for RNA extraction and RNA sequencing analysis of *D. melanogaster* S2 cells with or without insulin treatment or WNV-Kun infection (MOI 0.01 = PFU/cell). (B) GSEA using transcript levels for each experimental condition normalized to 0 μM insulin + mock infection from the RNAseq analysis. GO categories were selected based on GSEA *P* value ($P < 0.05$) for at least one experimental condition. (C) Venn Diagram of all transcripts enriched or suppressed for each experimental condition normalized to 0 μM insulin + mock infection. Transcripts were selected based on their $\log_2$(fold change) (FC) > ±1.5 and $P < 0.05$ for at least one experimental condition. (D) The number of genes transcriptionally enriched (yellow) or suppressed (blue) for each experimental condition normalized to 0 μM insulin + mock infection. (E) Hierarchal clustering and heat map expression of genes transcriptionally enriched or suppressed as identified in panels (C and D). Genes shown in enlarged cluster identify a subset of genes that showed the most up-regulation compared to no insulin treatment.

Gene set enrichment analysis (GSEA) was performed to identify and compare enriched gene sets in 0 μM insulin + WNV-Kun, 1.7 μM insulin + mock infection,

and 1.7 µM insulin +WNV-Kun (Fig. 1B; Table S2). Analysis was completed to identify previously unidentified gene sets for further analysis as well to compare to previous targeted qRT-PCR analysis showing enrichment of insulin and JAK/STAT signaling (13). Gene sets were filtered for $P < 0.05$ in at least one experimental condition and were selected based on their association with immunity and WNV disease (Table S2). We identified eight gene sets that are significantly enriched in the presence of insulin including immune response elements (response to oxidative stress, regulation of JAK-STAT cascade), canonical insulin signaling (phosphoinositide 3-kinase activity, insulin-like growth factor receptor signaling pathway, positive regulation of TOR signaling pathway, Ras protein signal transduction), and physiological development (establishment of glial blood-brain barrier, heart development). (Fig. 1B; Table S2).

Further analysis into the specific genes that were transcriptionally induced or suppressed was carried out to better understand the impact that infection or insulin treatment has on the *D. melanogaster* transcriptome. Genes were filtered for $P < 0.05$ and a $\log_2$(fold change) > ±1.5 for at least one experimental condition. There was a ~10-fold increase in the number of differentially expressed genes in cells that received insulin treatment and those that received no insulin (Fig. 1C and D). A total of 535 genes (520 genes shared between 1.7 µM insulin + mock infection and 1.7 µM insulin +WNV-Kun, and 15 genes shared among all three experimental groups) were commonly regulated in the presence of insulin regardless of WNV-Kun infection status (Fig. 1C). Together, this suggests that insulin treatment alters gene expression profiles with a high overlap in genes affected between mock infection and WNV-Kun infection. Cells that were not treated with insulin but were infected with WNV-Kun exhibited only 22 upregulated genes and 41 downregulated genes. Cells that received only insulin treatment reported 605 upregulated genes and 133 downregulated genes. Cells that received insulin treatment and WNV-Kun infection exhibited 551 upregulated genes and 127 downregulated genes (Fig. 1D). These results suggest that insulin treatment regulates a large set of genes during early stages of infection that can potentially impact later virus-specific responses.

Genes that were transcriptionally altered in Fig. 1C and D were used to generate a hierarchical clustering heatmap (Fig. 1E). As the goal of this study was to investigate effectors involved in insulin-mediated antiviral immunity, we were specifically interested in identifying and evaluating genes that were enriched in the presence of insulin treatment (Fig. 1E, expanded node; Table S1, Sheet 2). We selected genes for further analysis based on their function in immunity, insulin signaling, or that possess a putative ortholog in humans via DIOPT v8.5 (30) including *CG5326* (31), *TotF* (32), and *CG43775* (33). *CG5326* is a putative ortholog of ELOVL1/7 (31), which is demonstrated to contribute to human cytomegalovirus-mediated remodeling of the host lipidome (34). *TotF* is a humoral factor that responds to stress (32) and is induced during bacterial infection (35). *CG43775* is a putative ortholog of peptidase inhibitor 16 (PI16) (33), which is primarily associated with cardiovascular-related function (36, 37) but has been linked to insulin (38, 39) and T-cell function (39). Based on these established associations with host immunity or insulin signaling, we pursued these genes for subsequent analysis.

Survival of *D. melanogaster* that possesses gene disruption by transposable element insertion ($CG5326^{G6402}$ and $CG43775^{MB08418}$) or downregulation through RNAi (*TotF*) was assessed and compared to their respective controls. Female flies were mock- or WNV-Kun-infected with 5,000 PFU/fly, and survival was measured over 30 days. Hazard ratios were generated as a metric of host mortality, comparing mortality rates of virus- to mock-infected for the mutant flies and their respective controls (Fig. 2). *CG5326* mutants (Fig. 2B) exhibited similar mortality rates to virus infection than control flies (Fig. 2A). Conversely, *CG43775* (Fig. 2C) and *TotF* (Fig. 2D and E) mutants exhibited increased morality relative to their infected controls. Since the role of TotF has previously been linked to response to infection (35), we next investigated the role of CG43775 during WNV-Kun infection.

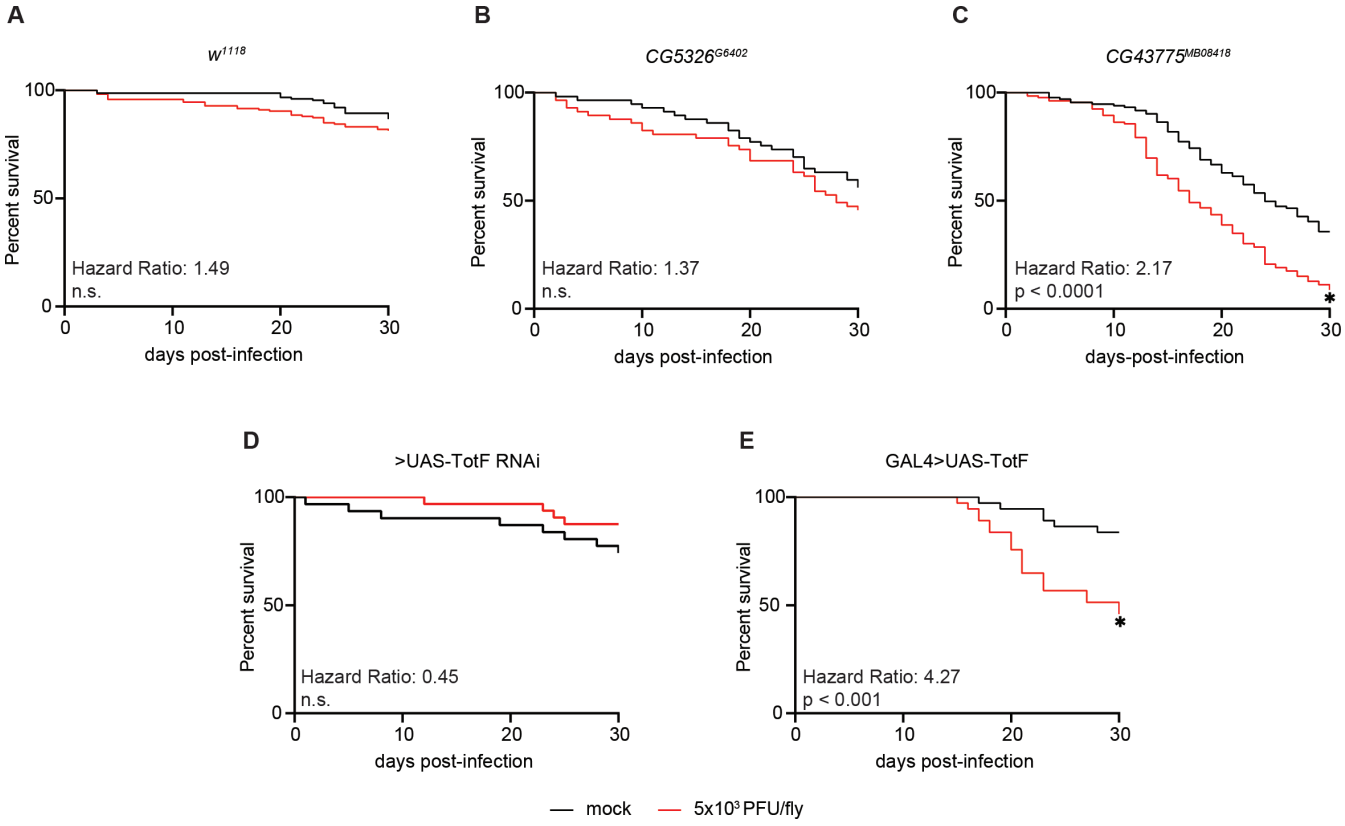

FIG 2 *CG43775*- and *TotF*-deficient flies are more susceptible to WNV-Kun infection. (A) Control w^{1118} and (B) *CG5326* mutant flies are not susceptible to WNV-Kun infection (red line) compared to mock infection (black line). (C) *CG43775*-infected flies exhibit increased mortality compared to mock infection. (D and E) Knockdown of *TotF* by RNAi shows that these flies exhibit increased mortality to WNV-Kun infection (F) whereas control flies do not (E). Each survival curve represents two (B–E) or four (A) independent experiments of >40 flies that were combined for a final survival curve (*$P < 0.01$, log-rank test).

D. melanogaster CG43775 contributes to insulin-mediated antiviral immunity

We sought to determine if *CG43775* is associated with insulin signaling and contributes to host immunity. We hypothesized that *CG43775*, similar to its human ortholog and other genes identified in Fig. 1E, may be important to host responses to WNV infection.

We observed significant induction of *CG43775* in *D. melanogaster* S2 cells with 1.7 µM insulin + WNV-Kun relative to other experimental conditions (Fig. 3A). To expand the role that *CG43775* has on host survival to viral infection (Fig. 2C), we measured viral titer in mutant and control flies at 1-, 5-, and 10 days post-infection (d p.i.) by standard plaque assay (Fig. 3B). We observed significantly higher virus replication in mutant flies by 10 d p.i. These data suggest that *CG43775* is important for host survival to WNV-Kun infection due to its ability to reduce virus replication. Due to the limited characterization of *CG43775*, it is possible that the observed difference in virus replication may be due to responses beyond immune signaling, which requires further analysis regarding how *CG43775* functions in insulin-mediated immunity.

Upon establishing that *CG43775* impacts host survival and WNV-Kun replication, we sought to examine the role of *CG43775* in insulin-mediated antiviral immunity. We fed mutant and control flies with 0 or 10 µM insulin 2 days prior to and during infection and collected flies at 1-, 5-, and 10 d p.i. to measure virus replication (Fig. 3C). Similar to the previous results, we observed that mutant flies had higher viral titers relative to the genetic control. We also observed that while insulin-treated control flies had a reduction in viral titers, there was no difference between 0 and 10 µM insulin-treated *CG43775* mutant flies. These results indicate that loss of *CG43775* expression results in a loss of insulin-mediated reduction in viral replication.

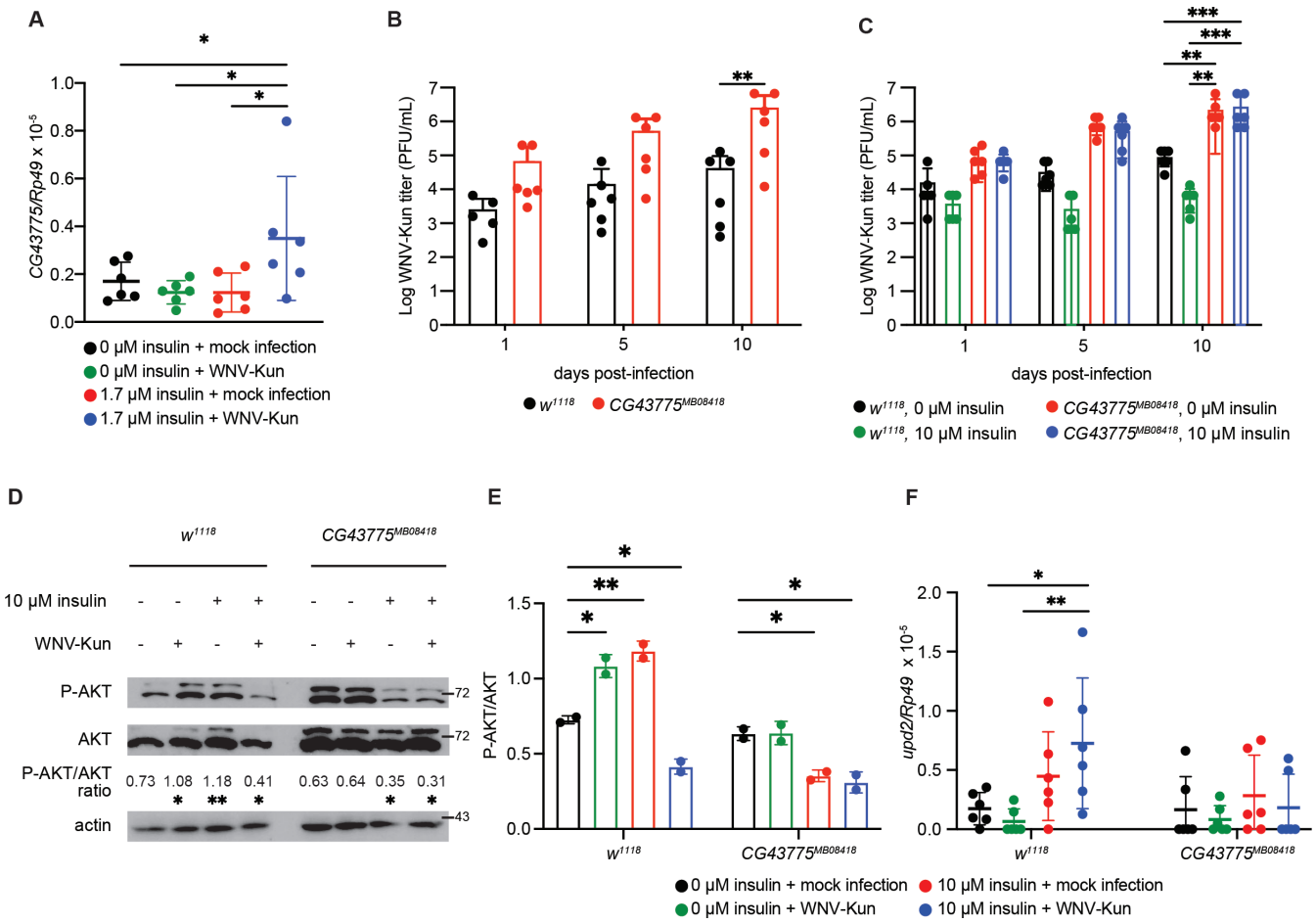

FIG 3 *CG43775* mutant flies exhibit increased WNV-Kun replication due to deficient insulin-mediated antiviral protection. (A) *CG43775* is induced in *D. melanogaster* S2 cells that were insulin-treated and WNV-Kun infected (*$P < 0.05$, one-way ANOVA). (B) WNV-Kun titer is higher in $CG43775^{MB08418}$ flies relative to w^{1118} genetic control by 10 d p.i. (**$P < 0.01$, two-way ANOVA). (C) Insulin treatment reduces WNV-Kun titer in control w^{1118} flies but not in $CG43775^{MB08418}$ flies (**$P < 0.01$, ***$P < 0.001$, two-way ANOVA). (D) AKT is phosphorylated and active in the presence of insulin for w^{1118} flies but not in $CG43775^{MB08418}$ flies at 5 d p.i. (*$P < 0.05$, **$P < 0.01$, one-way ANOVA). (E) Densitometry analysis of AKT phosphorylation shows that levels are diminished in insulin-treated *CG43775* mutant flies but not control flies relative to AKT (*$P < 0.05$, **$P < 0.01$, one-way ANOVA). (F) $CG43775^{MB08418}$ flies have impaired induction of *upd2* compared to genetic control w^{1118} flies. For qRT-PCR results, each circle represents individual biological replications consisting of individual wells (A) or pooled collection of three flies (F). For titer results (B and C), each circle represents individual biological replications consisting of a pooled collection of five flies. Titer and qRT-PCR results (B,C and F) are representative of triplicate independent experiments. Western blot results are representative of duplicate independent experiments of three to five flies per replicate (D and E).

To further dissect the role that *CG43775* has on insulin-mediated antiviral immunity, we sought to evaluate the impact that *CG43775* expression has on insulin signaling and JAK/STAT activation. Previous results demonstrate that insulin treatment of S2 cells activates AKT and JAK/STAT signaling, leading to the reduction of WNV-Kun (13). At 5 d p.i., we observed increased AKT phosphorylation in insulin-treated w^{1118} flies compared to *CG43775* mutant flies (Fig. 3D) and quantified using densitometry analysis (Fig. 3E). This leads us to conclude that *CG43775* mutant flies have a dysfunctional insulin signaling response that may impact insulin-mediated induction of antiviral JAK/STAT signaling. However, in the presence of insulin treatment and WNV-Kun infection, AKT phosphorylation was similar between genotypes, which may be due to virus-induced inhibition of AKT activation as previously observed in influenza-induced disruption of fatty acid synthesis and metabolic signaling in mouse models (40). Furthermore, w^{1118} flies that were treated with insulin and infected with WNV-Kun had diminished AKT phosphorylation compared to flies that received either insulin or WNV-Kun. This may be

caused by a secondary physiological signaling pathway or multiple pathways, which are absent *in vitro,* that impact AKT signaling and result in diminished AKT phosphorylation regardless of insulin treatment but remain sufficient to protect against WNV disease (41–43).

Due to the observed dysfunctional AKT signaling, we next sought to evaluate whether the expression of *CG43775* expression impacts downstream antiviral JAK/STAT signaling. Insulin treatment in S2 cells leads to the induction of unpaired (upd) cytokines and JAK/STAT activation (13). Thus, we examined *upd2* induction in control and *CG43775* mutant flies. At 5 d p.i., we observed significant induction of *upd2* in insulin-treated control flies, but not in *CG43775* mutant flies (Fig. 3F). Collectively, these data suggest that *CG43775*, a previously uncharacterized gene, contributes to activation of AKT and JAK/STAT signaling that leads to antiviral immunity during WNV-Kun infection.

Insulin and endothelin signaling reduce WNV-Kun replication in human HepG2 cells

One of the goals of our study was to determine whether results extrapolated from *D. melanogaster* could be used to analyze orthologous signaling pathways in humans. To achieve this goal, we performed gene ontology (GO) analysis using the PANTHER Classification System and genes from the cluster presented in Fig. 1E (44, 45). Using this gene set, only the endothelin signaling pathway was identified (Table S1, Sheet 3). Endothelin signaling is primarily associated with cardiovascular function and smooth muscle constriction (22, 46). Through this functional role, endothelin signaling also interacts and impacts associated components linked to insulin signaling including the PI3K/AKT/FOXO axis (28, 29, 47–51) and MAPK/ERK axis (52, 53) (Fig. 4A). The endothelin signaling pathway is not a canonical immune pathway; however, it has been linked to *Mycobacterium tuberculosis* (23) and hepatitis B/C virus infection (24, 54), which leads us to consider that endothelin signaling may also be involved during WNV infection and should be further analyzed.

The endothelin signaling pathway is not well-characterized in *D. melanogaster*; however, the pathway has been heavily dissected in mammals and permits us to investigate its potential role as an antiviral mediator to WNV-Kun in human cells. We selected to evaluate the endothelin signaling pathway as opposed to the specific human orthologs of CG43775, specifically PI16 and CLEC18 (30). Knockdown of these human genes did not impact insulin-mediated antiviral activity (data not shown). Additionally, based on the PANTHER GO analysis (Table S1, Sheet 3) and the broad influence that endothelin has on various signaling pathways linked to immunity (Fig. 4A), we examined the endothelin pathway to determine its impact on host responses to infection.

We first evaluated the extent to which insulin-mediated antiviral immunity functions in an *in vitro* human model system. Human HepG2 liver cells were treated with either 0 or 1.7 µM bovine insulin prior to and during WNV-Kun (MOI = 0.01 PFU/cell). Titer was measured at 1, 2, 3, and 5 d p.i. to determine if insulin similarly reduces viral titer as previously seen in insect cells (13, 41) (Fig. 4B). We observed that insulin treatment significantly reduces titer relative to non-treated cells by 2 d p.i. Similarly, we also measured viral titer at 2 d p.i. in HepG2 cells following 0, 1.7 µM bovine insulin, or 10 units/mL interferon (IFN)-β or -γ treatment and infected with WNV-Kun (MOI = 0.01 PFU/cell) (Fig. 3C). IFN treatment is known to reduce WNV replication in human cells (55–59), so this comparison was to determine the efficacy of insulin in reducing WNV-Kun replication. We observed that insulin, like IFN treatment, significantly reduced viral replication compared to mock treatment at 2 d p.i. and that IFN-β exhibited the greatest magnitude of reduction (60).

Upon establishing that insulin treatment reduces WNV-Kun in HepG2 cells, similar to that we observed in flies, we next sought to evaluate whether an endothelin-dependent mechanism was occurring in the mammalian model. To investigate endothelin signaling in mammalian insulin-mediated antiviral immunity, we measured induction of the ligand *endothelin 1* (*EDN1*) in HepG2 cells during WNV-Kun infection and insulin treatment (Fig.

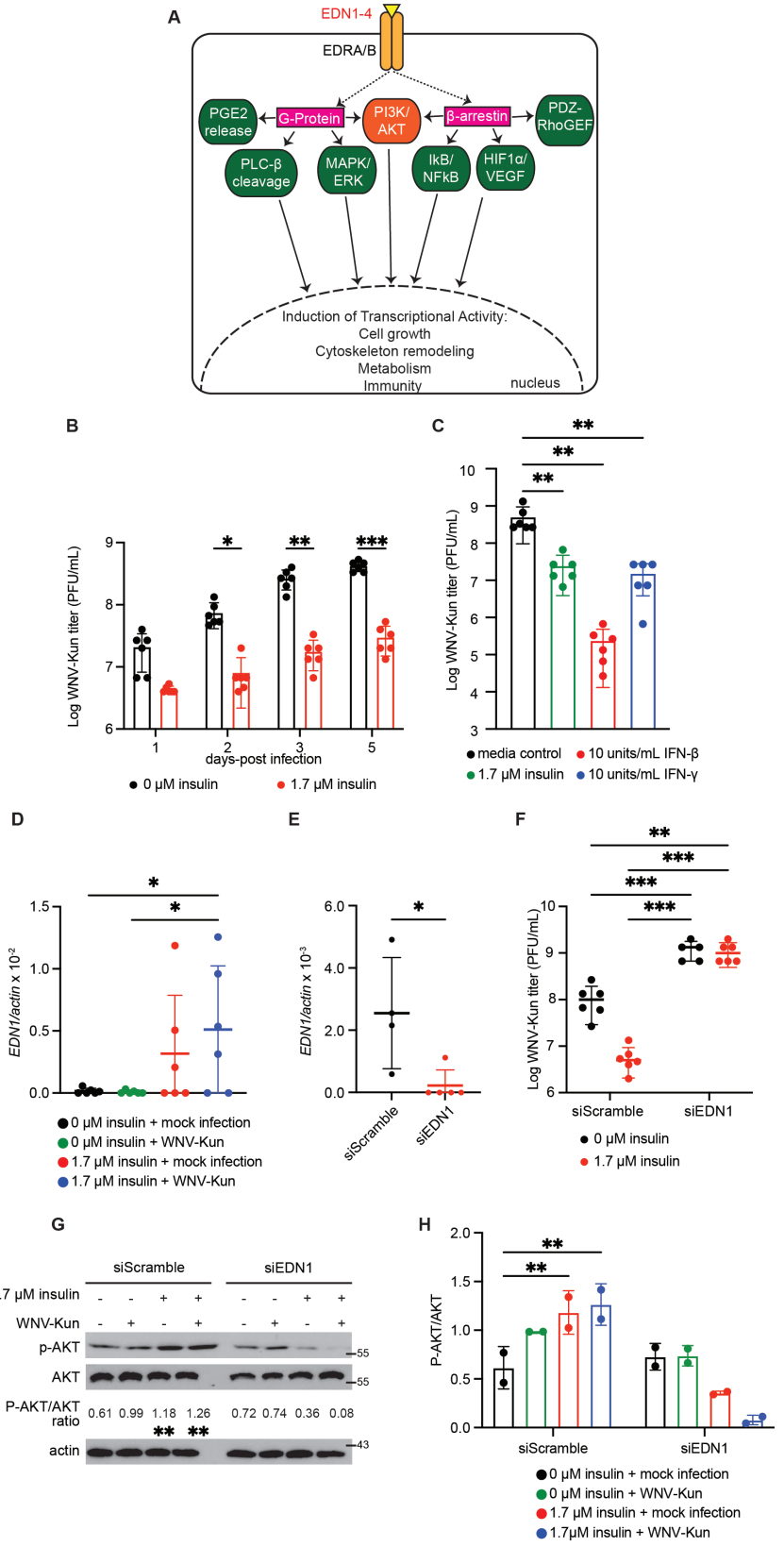

FIG 4 Endothelin signaling is antiviral to WNV-Kun through an insulin-dependent mechanism in human HepG2 cells. (A) Schematic of canonical endothelin signaling in mammals and its intracellular and

(Continued on next page)

FIG 4 (Continued)

transcriptional activity. (B) Insulin treatment of HepG2 cells reduces WNV-Kun titer (MOI = 0.01 PFU/cell) (*P < 0.05, **P < 0.01, ***P < 0.001, two-way ANOVA). (C) WNV-Kun titer at 2 d p.i. is reduced in cells that received either 1.7 µM insulin, 10 units/mL IFN-β, or 10 units/mL IFN-γ treatment 24 h prior to infection (MOI = 0.01 PFU/cell) (**P < 0.01, one-way ANOVA). (D) *EDN1* is induced in insulin-treated and WNV-Kun-infected HepG2 cells (*P < 0.05, one-way ANOVA). (E and F) *EDN1* was knocked down in HepG2 cells (E) (*P < 0.05, unpaired *t*-test) 48 h prior to insulin treatment and WNV-Kun infection, and viral titer was measured by standard plaque assay at 2 days post infection. (F) (**P < 0.01, ***P < 0.001, two-way ANOVA). (G and H) Insulin-mediated AKT phosphorylation is decreased in the absence of *EDN1* as measured by densitometry analysis (**P < 0.01, one-way ANOVA). Circles represent individual biological replications. Horizontal bars represent the mean. Error bars represent SDs. Titer and qRT-PCR results (B–F) are representative of triplicate independent experiments. Western blot results are representative of duplicate independent experiments (G and H).

4D). We observed significant induction of *EDN1* in the presence of insulin and during WNV-Kun infection in the presence of insulin. This indicates that like our previous observations in *D. melanogaster*, endothelin signaling may be involved in insulin-mediated antiviral immunity in human cells. To further evaluate this hypothesis, we transfected HepG2 cells with either non-targeting control siRNA (siScramble) or EDN1 siRNA (siEDN1) (Fig. 4E). We observed a 91% reduction in *EDN1* expression in cells transfected with siEDN1. We then insulin-treated and infected cells knocked down for EDN1 to measure viral replication at 2 d p.i. In cells knocked down for EDN1 and treated with insulin, we observed that while the siScramble control cells maintain a reduction in WNV-Kun replication in the presence of insulin, we lose this insulin-mediated antiviral protection when EDN1 expression is diminished (Fig. 4F). We also observed a significant increase in overall WNV-Kun replication even in the absence of insulin treatment. It is likely that endothelin signaling contributes to host responses to control infection that may be independent of insulin as we see an increase in WNV-Kun replication even when EDN1 is knocked down. Taken together, endothelin signaling may be connected with the insulin-mediated antiviral response previously observed by others in a mammalian model (61–64).

We next tested the role that *EDN1* expression has on insulin signaling by measuring phosphorylation of AKT in HepG2 cells following insulin treatment and WNV-Kun infection at 2 d p.i. These cells were also transfected with siScramble or siEDN1 prior to treatment and infection (Fig. 4G). We observed that control cells had higher expression of P-AKT in the presence of insulin and infection, while the loss of EDN1 had diminished P-AKT expression regardless of insulin treatment (Fig. 4G) and it was quantified using densitometry analysis (Fig. 4H). This further connects endothelin as a novel mediator of antiviral protection through an insulin-specific mechanism.

Insulin- and endothelin-mediated signaling is antiviral to virulent WNV-NY99

Previous analysis of insulin-mediated antiviral immunity in an insect (13) and present mammalian context has used the attenuated Kunjin subtype of WNV. While useful in dissecting and evaluating host immunity to WNV in a general context, a present limitation is that this strain causes limited disease in immune-competent human hosts. This is due to a number of factors including increased sensitivity to type I interferon responses (65) and decreased efficacy in antagonizing JAK/STAT signaling due to a mutation in the NS5 protein (56). Because of this limitation regarding clinical relevance, we sought to evaluate whether insulin-mediated antiviral protection was present against more virulent strains and if so the impact that endothelin signaling possesses for regulating viral replication. Like previous experiments, we used HepG2 cells that received either 0 or 1.7 µM insulin treatment 24 h prior to and during WNV-NY99 (MOI = 0.01 PFU/cell) infection and measured viral titer at 1, 2, 3, and 5 d p.i. (Fig. 5A). We observed that WNV-NY99 titer was reduced in cells that received insulin treatment. We also observed overall higher virus titer in WNV-NY99-infected cells compared to WNV-Kun-infected

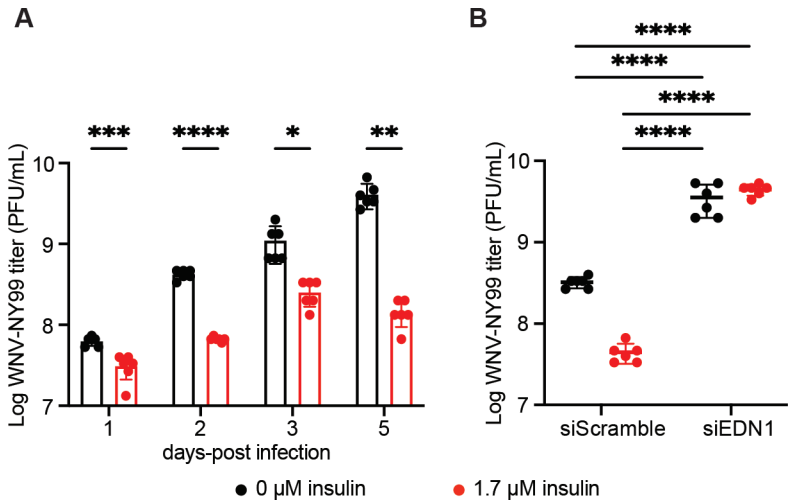

FIG 5 Endothelin and insulin-mediated signaling is conserved against more virulent WNV-NY99 strain in HepG2 cells. (A) Insulin treatment reduces WNV-NY99 titer (MOI = 0.01 PFU/cell) (*P < 0.05, **P < 0.01, ***P < 0.001, ****P < 0.0001, two-way ANOVA). (B) siRNA silencing of EDN1 results in increased WNV-NY99 viral replication and loss of insulin-mediated protection compared to non-specific siScramble control at 2 days post-infection (****P < 0.0001, two-way ANOVA). Circles represent individual biological replications. Horizontal bars represent the mean. Error bars represent SDs. Results are representative of triplicate independent experiments.

cells. Because of the established link that insulin signaling induces JAK/STAT in mammals (66, 67) and insects (13), this increase in overall viral titer is likely due to the enhanced antagonism WNV-NY99 can successfully initiate as opposed to the attenuated WNV-Kun strain (56, 65). We followed up this analysis by measuring WNV-NY99 titer in HepG2 cells that received either non-targeting or EDN1 siRNA (Fig. 5B). We observed a similar loss of insulin-mediated protection and increased viral load in siEDN1-transfected cells, which was previously observed during WNV-Kun infection. This observation ultimately leads us to conclude that downstream components of insulin-mediated antiviral immunity, specifically endothelin signaling, play a role in reducing WNV replication for both attenuated and more virulent strains that may be a potential target for future clinical or therapeutic research.

DISCUSSION

Arbovirus infections are a growing health threat that requires more effective means of intervention both environmentally (i.e., vector transmission) and clinically. While our ability to develop more effective vector control protocols has improved, the ability to understand and clinically address human infections and severe diseases remains underdeveloped. As WNV, along with other mosquito-borne diseases, continues to expand in both global distribution and incidence (5, 7, 68, 69), the need for effective preventatives and treatments is more urgent than ever. Human vaccine development against WNV has made limited progress (70), so development of effective antivirals post exposure is necessary.

In the study presented here, we highlight the genetic power of *D. melanogaster* to advance the study of antiviral immunity and identify components of insect and mammalian host responses that regulate WNV infection. We demonstrate that insulin induces several genes and signaling pathways that are both canonical and previously unidentified antiviral mediators (Fig. 1). Our study using the *D. melanogaster* model identifies roles in insulin and immunity for previously uncharacterized genes associated, specifically regarding host survival and viral replication in the insect (Fig. 2 and 3). We also demonstrate that we can use these results to translate our findings into the more pertinent human model and under-characterized endothelin signaling pathway (Fig. 4).

In addition, we demonstrate that our findings are applicable to the more virulent and clinically relevant WNV strain NY99 (Fig. 5).

In our study, we show that dysfunctional endothelin signaling results in increased host mortality and WNV replication. However, further investigation is also necessary to evaluate its role during infection. Like insulin, endothelins are linked to various physiological processes like cardiovascular health so induction of this pathway, while potentially antiviral, may impact other off-target processes. Increased production and secretion of EDN1 have been used as indicators for oncogenic and virus-induced hepatocellular carcinoma (24, 54, 71) as a promoter of cell growth and proliferation while inhibiting pro-apoptotic signaling (72). EDN1 expression is also proposed as a biomarker for patients receiving interferon-α treatment as elevated levels can be used to infer progression to interferon-induced pulmonary toxicity (27). In relation to insulin sensitivity and signaling, serum EDN1 is elevated in diabetic individuals who later develop diabetic microangiopathy and nephropathy that progresses to more advanced insulin resistance (73, 74). Additional concerns are apparent as endothelin signaling, while antiviral in this study, may promote or enhance infection against other pathogens. *Mycobacterium tuberculosis* secretes the protease enzyme Zmp1 that cleaves EDN1 and activates endothelin signaling that promotes bacteria survival within the lungs (23). Thus, further investigation is needed to understand how targeting the endothelin pathway influences other related viruses that are either targeted by or disrupt insulin signaling in the presence or absence of WNV infection.

Determining the overall effect that insulin-mediated protection and endothelin signaling has in a clinical context will be important if targeting the pathways are used as an intervention for WNV disease. It is unlikely that administering insulin to a patient alone is a viable approach for treating WNV since it can influence a number of off-target physiological processes and may lead to further insulin resistance or disease pathology (18, 19). Instead, we propose through our study that by targeting pathways downstream of insulin signaling, we can effectively and directly induce more potent antiviral responses with limited toxicity to the host. While our study focused on endothelin signaling, there were other gene sets and associated pathways identified in our RNAseq screen, which are worth further investigation regarding their potential role in antiviral immunity.

Taken together, our study identifies a novel component of insect and human antiviral immunity and expands our current understanding regarding insulin-mediated responses to infection. Previous investigation demonstrated that a variety of viruses including influenza (40), WNV (61, 75), and ZIKV (20, 76) target and disrupt host processes associated with insulin signaling. Typically, insulin signaling disruption results in metabolic dysfunction that can cause more severe morbidity and mortality. Here, we demonstrate that targeting insulin signaling protects fruit flies and humans from increased viral replication. Additionally, we show that endothelin signaling provides antiviral immunity to WNV. While endothelins have been heavily dissected as a regulator of cardiovascular health and vasoconstriction (27, 28, 52), they also possess a role in hepatic (24, 48, 54, 71) and neuronal (77–80) regulation and health. Importantly, endothelin signaling is dependent on its different isoforms as they relate to their specific receptors on different cell types and physiological functions (22). WNV disease is heavily associated with encephalitis and neurodegenerative disease (81, 82). Because EDN1 has been linked to virus-induced demyelinating disease (77) and promotes anti-inflammatory signaling in circulating immune cells (26), endothelin signaling may also function as an antiviral target and determinant in severe WNV disease progression and is worth further investigation.

Given the conservation of insulin signaling and its activation during viral infection across insect and mammalian species, downstream targets of insulin or endothelin signaling may have a broader role within an antiviral context. If possible, it may provide a means of more effectively responding to these growing pathogens of concern while

also limiting potential complications associated with current intensely robust antiviral therapeutics.

MATERIALS AND METHODS

Fly lines and rearing

Drosophila lines were obtained through the Bloomington Drosophila Stock Center. Lines used include wild-type control lines w^{1118} (BDSC: 5905); actin driver line: y^1w^*; *P{w[+mC]=Act5 C-GAL4}25FO1/CyO,y*$^+$ (BSDC: 4414); *TotF* RNAi (83): *y1sc***v1sev21; P{TRiP.HMC06169}attP40* (BSDC: 65906); *CG5326* mutant (84): w1118; P{EP}CG5326G6402 (BSDC: 32024); and *CG43775* mutant (84): w1118; Mi{ET1} CG3257MB08418 CG43775MB08418 CG43776MB08418 CG43777MB08418 (BSDC: 26113).

Flies were maintained on standard cornmeal food (Genesee Scientific #66-112) at 25°C and 65% relativity humidity, and a 12 h/12 h light/dark cycle. Flies are negative for *Wolbachia* infection. Female adult flies used for all experiments were 2–7 days post-eclosion. For insulin treatment, cornmeal food was supplemented with 10 µM bovine insulin (Sigma-Aldrich I6634) and flies were maintained on food 48 h prior to and during infection as described (13).

Cells and virus

Vero cells (ATCC, CCL-81) were provided by A. Nicola and cultured at 37°C/5% CO_2 in Dulbecco's modified Eagle medium (DMEM) (ThermoFisher 11965) supplemented with 10% fetal bovine serum (FBS) (Atlas Biologicals FS-0500-A) and 1× antibiotic-antimycotic (ThermoFisher 15240062). S2 cells were provided by L. Cherbas and cultured as described (85) and are negative for Flock House virus. HepG2 cells (ATCC, HB-8065) were provided by M. Konkel and cultured at 37°C/5% CO_2 in DMEM supplemented with 10% FBS. For insulin treatment, culture media with 2% FBS were supplemented with 1.7 µM bovine insulin (Sigma-Aldrich I6634) as described (86). For interferon-β and -γ treatment, 2% FBS in DMEM media was supplemented with 10 units/mL of either IFN-β (Sigma-Aldrich IF014) or IFN-γ (Sigma-Aldrich IF002) for 24 h prior to infection as described (60).

West Nile virus-Kunjin strain MRM16 (WNV-Kun) was gifted by R. Tesh and propagated in Vero cells. West Nile virus strain 385-99 (WNV-NY99) was obtained by BEI Resources, NIAID, NIH (NR-158) and propagated in Vero cells. All experiments with a specific virus type utilized the same stock.

RNA isolation, library preparation, and RNA sequencing

D. melanogaster S2 cells were treated with 0 or 1.7 µM bovine insulin for 24 h. Cells were then either mock-infected or infected with WNV-Kun (MOI = 0.01 PFU/cell) for 8 h. Total RNA was extracted from three individual wells using Direct-zol (Zymo Research, Irvine, CA, USA) following the manufacturer's instructions. Following total RNA extraction, the integrity of total RNA was assessed using Fragment Analyzer (Advanced Analytical Technologies, Ankeny, IA, USA) with the High Sensitivity RNA Analysis Kit. RNA Quality Numbers (RQNs) from 1 to 10 were assigned to each sample to indicate its integrity or quality. "10" stands for a perfect RNA sample without any degradation, whereas "1" marks a completely degraded sample. RNA samples with RQNs ranging from 8 to 10 were used for RNA library preparation with the TruSeq Stranded mRNA Library Prep Kit (Illumina, San Diego, CA, USA). Briefly, mRNA was isolated from 2.5 µg of total RNA using poly-T oligo attached to magnetic beads and then subjected to fragmentation, followed by cDNA synthesis, dA-tailing, adaptor ligation, and PCR enrichment. The sizes of RNA libraries were assessed by Fragment Analyzer with the High Sensitivity NGS Fragment Analysis Kit. The concentrations of RNA libraries were measured by StepOnePlus Real-Time PCR System (ThermoFisher Scientific, San Jose, CA, USA) with the KAPA Library Quantification Kit (Kapabiosystems, Wilmington, MA, USA). The libraries were

diluted to 2 nM in 10 mM Tris-HCl, pH 8.5, and denatured with 0.1 N NaOH. Eighteen pM libraries were clustered in a high-output flow cell using HiSeq Cluster Kit v4 on a cBot (Illumina). After cluster generation, the flow cell was loaded onto HiSeq 2500 for sequencing using HiSeq SBS kit v4 (Illumina). DNA was sequenced from both ends (paired-end) with a read length of 100 bp. The raw bcl files were converted to fastq files using the software program bcl2fastq2.17.1.14. Adaptors were trimmed from the fastq files during the conversion. On average, 40 million reads were generated for each sample. RNA sequencing was performed at the Spokane Genomics CORE at Washington State University-Spokane in Spokane, WA, USA.

Bioinformatics analysis

RNA-seq reads were imported and aligned using Qiagen CLC Genomics Workbench (Version 11.0.1) to the *D. melanogaster* genomic reference sequence. Reads for each biological replicate within an experimental condition were pooled and averaged. Differential expression of transcript levels for each experimental condition (WNV-Kun infection, insulin treatment, or both infection and treatment) were normalized to reads for cells that received neither treatment nor infection. Transcripts were filtered for *P*-values less than or equal to 0.05 and a $\log_2$(fold change) > ±1.5 for at least one experimental condition.

Filtered transcripts were imported into TIBCO Spotfire Analytics (Version 1.1.3) for gene clustering and heatmap generation. Gene clustering was performed using hierarchical clustering using UPGMA (unweighted pair group method with arithmetic mean) with Euclidean distance with ordering weight set to average value and normalization by mean. GSEA was performed as previously described (87) using a cutoff of $P < 0.05$ for at least one experimental condition for GO classifications (87–89). Highlighted classifications are shown in Fig. 1B. *Drosophila* gene ontologies were imported from FlyBase (version fb_2016_04) as previously described (90). Further GO analysis for genes clustered and presented in Fig. 1E used PANTHER GO-Slim (Version 14.0) to identify the endothelin signaling pathway as an overrepresented GO category.

Fly infections

Two-to-seven-day old adult female *D. melanogaster* were anesthetized with CO_2 and injected intrathoracically with WNV-Kun with 5,000 PFU/fly, as previously described (12, 90). Mock-infected flies received equivalent volume of PBS. For mortality studies, groups of 30–50 flies were injected and maintained on cornmeal food for 30 days. All survival studies were repeated at least twice and survival data were combined. Fly food vials were changed every 2–3 days. For viral titration experiments, three groups of four to five flies were collected, homogenized in PBS, and used as individual samples for plaque assay as described in reference (13). For qRT-PCR and Western blot experiments, three groups of three to five flies were collected at 5 d p.i., homogenized in Trizol or radioimmunoprecipitation assay buffer (RIPA), respectively, and centrifuged to isolate and remove the cuticle. The supernatant was collected and used for further analysis.

In vitro virus replication

HepG2 cells were seeded into a 24-well plate at a confluency of 1.25×10^5 cells/well with six independent wells for each experimental condition. The following day, cells were treated with either 1.7 µM bovine insulin or acidified water in 2% FBS in DMEM for 24 h prior to infection. For measuring viral replication following interferon treatment, 2% FBS in DMEM media was supplemented with 10 units/mL of either IFN-β or IFN-γ for 24 h prior to infection as described (60). Cells were then infected with WNV-Kun or WNV-NY99 at an MOI of 0.01 PFU/cell for 1 h. The virus inoculum was removed, and fresh experimental media was added. Supernatant samples were collected at 1, 2, 3, and 5 d p.i. for later titration. WNV titers were determined by standard plaque assay on Vero cells.

Immunoblotting

Protein extracts were prepared by lysing cells or flies with RIPA buffer (25 mM Tris-HCl pH 7.6, 150 mM NaCl, 1 mM EDTA, 1% NP-40, 1% sodium deoxycholate, 0.1% SDS, 1 mM Na_3VO_4, 1 mM NaF, 0.1 mM phenylmethylsulfonyl fluoride(PMSF), 10 µM aprotinin, 5 µg/mL leupeptin, 1 µg/mL pepstatin A). Protein samples were diluted using 2× Laemmli loading buffer, mixed, and boiled for 5 minutes at 95°C. Samples were analyzed by SDS/PAGE using a 10% acrylamide gel, followed by transfer onto polyvinylidene difluoride (PVDF)membranes (Millipore IPVH00010). Membranes were blocked with 5% BSA (ThermoFisher BP9706) in Tris-buffered saline (50 mM Tris-HCl pH 7.5, 150 mM NaCl) and 0.1% Tween-20 for 1 h at room temperature.

Primary antibody labeling was completed with anti-P-Akt (1:1,000; Cell Signaling 4060), anti-Akt (pan) (1:2,000) (Cell Signaling 4691), or anti-actin (1:10,000; Sigma A2066) overnight at 4°C. Secondary antibody labeling was completed using anti-rabbit IgG-HRP conjugate (1:10,000; Promega W401B) by incubating membranes for 2 h at room temperature. Blots were imaged onto a film using luminol enhancer (ThermoFisher 1862124). The P-AKT/AKT ratio for each experimental condition was determined using densitometry analysis using BioRad Image Lab (Version 6.1) comparing band intensity of P-AKT to AKT. The reported P-AKT/AKT ratio is the mean of duplicate independent experiments.

RNA interference *in vitro*

Double-stranded RNA (dsRNA) targeting human *EDN1* (Horizon Discovery J-016692-05-005) and non-targeting control (siScramble) dsRNA (Horizon Discovery D-001810-10-05) was transfected into HepG2 cells for 48 h prior to insulin treatment and infection as described (85). Total RNA was extracted and purified to confirm reduced expression by qRT-PCR.

Quantitative reverse transcriptase PCR

qRT-PCR was used to measure mRNA levels in *D. melanogaster* S2 cells, adult flies, and human HepG2 cells. Cells or flies were lysed with Trizol Reagent (ThermoFisher 15596). RNA was isolated by column purification (ZymoResearch R2050), DNase treated (ThermoFisher 18068), and cDNA was prepared (BioRad 170-8891). Expression of *D. melanogaster CG43775* (forward: CTGCAACAACAAGACGCACA; reverse: GAACTTGGTCGAGTTCCCGT) and *upd2* (forward: CCTATCCGAACAGCAATGGT; reverse: CTGGCGTGTGAAAGTTGAGA) (13) was measured using SYBR Green reagents (ThermoFisher K0222) and normalized to *Rp49* (forward: CCACCAGTCGGATCGATATGC; reverse: CTCTTGAGAACGCAGGCGACC) (91) to measure endogenous gene levels for all treatment conditions. Expression of human *EDN1* was measured using the probe for *EDN1* (Hs00174961_m1 ThermoFisher 4331182) and primers (forward: CAGGGCTGAAGACATTATGGAGA; reverse: CATGGTCTCCGACCTGGTTT) (92) and normalized to β-actin (Hs01060665_g1 ThermoFisher 4331182) using TaqMan Universal Master Mix (ThermoFisher 4304437). The reaction for samples included one cycle of denaturation at 95°C for 10 minutes, followed by 50 cycles of denaturation at 95°C for 15 seconds and extension at 60°C for 1 minute, using an Applied Biosystems 7500 Fast Real Time PCR System. ROX was used as an internal control.

Quantification and statistical analysis

Results presented as dot plots show data from individual biological replicates (n = 2–6), the arithmetic mean of the data shown as a horizontal line, and error bars representing standard deviations (SDs) from the mean. RNAseq read numbers were averaged among technical replicates (n = 2) with biological replicates (n = 3) used for each experimental condition using CLC Genomics Workbench analysis using a generalized linear model. *P*-values were calculated using a Wald test. GSEA *P*-values were calculated using false

discovery rate(FDR) as previously described (87–89). Biological replicates of adult *D. melanogaster* (n = 6–40) consisted of at least duplicate pooled flies. The results shown are representative of at least duplicate independent experiments, as indicated in the figure legends. All statistical analyses of biological replicates were completed using GraphPad Prism (Version 9) and significance was defined as $P < 0.05$. Ordinary one-way ANOVA with uncorrected Fisher's least significant difference(LSD) for multiple comparisons was used for qRT-PCR analysis. Two-way ANOVA with Šidák correction for multiple comparisons was used for multiday viral titer analysis and for siRNA viral titer analysis. One-way ANOVA with Šidák correction for multiple comparisons was used for single-day viral titer in the presence of insulin and interferon-β and -γ analysis. Two-tailed unpaired *t*-test was used for qRT-PCR validation of the knocked-down expression of *EDN1*. Repeated measures one-way ANOVA with uncorrected Fisher's LSD for multiple comparison was used for densitometry analysis. All error bars represent SD of the mean. Outliers were identified using a ROUT test (Q = 5%) and removed.

ACKNOWLEDGMENTS

We thank A. Nicola, M. Konkel, and R. Tesh for cells and viruses used in this study. We also thank the Spokane Genomics CORE at Washington State University for their preparation and guidance in the RNAseq analysis. We would like to thank S. Luckhart for constructive feedback regarding experimental direction and interpretation.

This research was supported by the WSU College of Veterinary Medicine Stanley L. Adler research fund, NIH/National Institute of General Medical Sciences (NIGMS)-funded pre-doctoralpre-doctoral fellowship (T32 GM008336) and a Poncin Fellowship to C.E.T. and L.R.H.A., NIH/NIGMS pre-doctoralpre-doctoral fellowship T32 GM008336, WSU Research Assistantships for Diverse Scholars (RADS), and ARCS Foundation Fellowship to B.J.J., The funders had no role in study design, data collection and analysis, decision to publish, or preparation of the manuscript.

The study was conceptualized by C.E.T., L.R.H.A., and A.G.G.; the methodology was designed by C.E.T., L.R.H.A., and A.G.G.; validation was done by C.E.T., E.H.R., B.J.J., A.B.C., S.F., and A.G.G..; C.E.T., E.H.R., B.J.J., A.B.C., S.F., L.R.H.A., and A.G.G. helped with the investigation; A.G.G. helped with the resources; C.E.T. was involved in the writing of original draft; the manuscript was reviewed and edited by E.H.R., B.J.J., L.R.H.A., A.B.C., S.F., and A.G.G.; C.E.T. and A.G.G. visualized the study; funding was acquired by C.E.T., B.J.J., L.H.R.A., and A.G.G.

The authors have declared that no competing interests exist.

AUTHOR AFFILIATIONS

[1]School of Molecular Biosciences, College of Veterinary Medicine, Washington State University, Pullman, Washington, USA
[2]RNA Viruses Section, Laboratory of Infectious Diseases, National Institute of Allergy and Infectious Diseases, National Institutes of Health, Bethesda, Maryland, USA
[3]Paul G. Allen School for Global Health, College of Veterinary Medicine, Washington State University, Pullman, Washington, USA

AUTHOR ORCIDs

Chasity E. Trammell http://orcid.org/0000-0002-1698-883X
Alan G. Goodman http://orcid.org/0000-0001-6394-332X

FUNDING

Funder	Grant(s)	Author(s)
Washington State University College of Veterinary Medicine Stanley L. Adler Research Fund		Alan G. Goodman
NIH/ NIGMS-funded predoctoral fellowship	T32 GM008336	Chasity E. Trammell

Funder	Grant(s)	Author(s)
		Brianne J. Jones
		Laura R. H. Ahlers
Poncin Fellowship		Chasity E. Trammell
		Laura R. H. Ahlers
WSU Research Assistantships for Diverse Scholars		Brianne J. Jones
ARCS Foundation Fellowship		Brianne J. Jones

AUTHOR CONTRIBUTIONS

Chasity E. Trammell, Conceptualization, Data curation, Formal analysis, Funding acquisition, Investigation, Methodology, Software, Supervision, Validation, Visualization, Writing – original draft, Writing – review and editing | Evelyn H. Rowe, Investigation, Validation, Writing – review and editing | Aditya B. Char, Investigation, Validation, Writing – review and editing | Brianne J. Jones, Investigation, Validation, Writing – review and editing | Stephen Fawcett, Investigation, Validation, Writing – review and editing | Laura R. H. Ahlers, Conceptualization, Visualization, Writing – review and editing | Alan G. Goodman, Conceptualization, Data curation, Formal analysis, Funding acquisition, Investigation, Methodology, Project administration, Resources, Software, Supervision, Validation, Visualization, Writing – review and editing

DATA AVAILABILITY

Raw and processed RNAseq data have been deposited in NCBI Gene Expression Omnibus (GEO) accession # GSE216532.

ADDITIONAL FILES

The following material is available online.

Supplemental Material

Table S1 (JVI01112-23-s0001.xlsx). Summary of RNAseq reads (Sheet 1), PANTHER GO analysis results (Sheet 2), and expression values of selected gene cluster (Sheet 3) (related to Fig. 1).
Supplemental table captions (JVI01112-23-s0002.docx). Captions for Tables S1 and S2.
Table S2 (JVI01112-23-s0003.xlsx). GO classifications ($P < 0.05$) and associated genes in 0 µM + WNV-Kun cells (Sheets 1-2), 1.7 µM insulin + mock infected cells (Sheets 3-4), and 1.7 µM insulin + WNV-Kun cells (Sheets 5-6) following GSEA (related to Fig. 1B).

REFERENCES

1. Ahlers LRH, Goodman AG. 2018. The immune responses of the animal hosts of West Nile virus: a comparison of insects, birds, and mammals. Front Cell Infect Microbiol 8:96. https://doi.org/10.3389/fcimb.2018.00096
2. Centers for Disease Control and Prevention (CDC). 1999. Outbreak of West Nile-like viral encephalitis--New York, 1999. MMWR Morb Mortal Wkly Rep 48:845–849.
3. Nash D, Mostashari F, Fine A, Miller J, O'Leary D, Murray K, Huang A, Rosenberg A, Greenberg A, Sherman M, Wong S, Layton M, 1999 West Nile Outbreak Response Working Group. 2001. The outbreak of West Nile virus infection in the New York City area in 1999. N Engl J Med 344:1807–1814. https://doi.org/10.1056/NEJM200106143442401
4. Lanciotti RS, Roehrig JT, Deubel V, Smith J, Parker M, Steele K, Crise B, Volpe KE, Crabtree MB, Scherret JH, Hall RA, MacKenzie JS, Cropp CB, Panigrahy B, Ostlund E, Schmitt B, Malkinson M, Banet C, Weissman J, Komar N, Savage HM, Stone W, McNamara T, Gubler DJ. 1999. Origin of the West Nile virus responsible for an outbreak of encephalitis in the Northeastern United States. Science 286:2333–2337. https://doi.org/10.1126/science.286.5448.2333
5. Gorris ME, Bartlow AW, Temple SD, Romero-Alvarez D, Shutt DP, Fair JM, Kaufeld KA, Del Valle SY, Manore CA. 2021. Updated distribution maps of predominant Culex mosquitoes across the Americas. Parasit Vectors 14:547. https://doi.org/10.1186/s13071-021-05051-3
6. Harrigan RJ, Thomassen HA, Buermann W, Smith TB. 2014. A continental risk assessment of West Nile virus under climate change. Glob Chang Biol 20:2417–2425. https://doi.org/10.1111/gcb.12534
7. Ludwig A, Zheng H, Vrbova L, Drebot MA, Iranpour M, Lindsay LR. 2019. Increased risk of endemic mosquito-borne diseases in Canada due to climate change. Can Commun Dis Rep 45:91–97. https://doi.org/10.14745/ccdr.v45i04a03
8. Evans BR, Kotsakiozi P, Costa-da-Silva AL, Ioshino RS, Garziera L, Pedrosa MC, Malavasi A, Virginio JF, Capurro ML, Powell JR. 2019. Transgenic Aedes aegypti mosquitoes transfer genes into a natural population. Sci Rep 9:13047. https://doi.org/10.1038/s41598-019-49660-6

9. Hedges LM, Brownlie JC, O'Neill SL, Johnson KN. 2008. Wolbachia and virus protection in insects. Science 322:702. https://doi.org/10.1126/science.1162418
10. Trammell CE, Ramirez G, Sanchez-Vargas I, St Clair LA, Ratnayake OC, Luckhart S, Perera R, Goodman AG. 2022. Coupled small molecules target RNA interference and JAK/STAT signaling to reduce Zika virus infection in Aedes aegypti. PLoS Pathog 18:e1010411. https://doi.org/10.1371/journal.ppat.1010411
11. Alli A, Ortiz JF, Atoot A, Atoot A, Millhouse PW. 2021. Management of West Nile encephalitis: an uncommon complication of West Nile virus. Cureus 13:e13183. https://doi.org/10.7759/cureus.13183
12. Yasunaga A, Hanna SL, Li J, Cho H, Rose PP, Spiridigliozzi A, Gold B, Diamond MS, Cherry S. 2014. Genome-wide RNAi screen identifies broadly-acting host factors that inhibit arbovirus infection. PLoS Pathog 10:e1003914. https://doi.org/10.1371/journal.ppat.1003914
13. Ahlers LRH, Trammell CE, Carrell GF, Mackinnon S, Torrevillas BK, Chow CY, Luckhart S, Goodman AG. 2019. Insulin potentiates JAK/STAT signaling to broadly inhibit Flavivirus replication in insect vectors. Cell Rep 29:1946–1960. https://doi.org/10.1016/j.celrep.2019.10.029
14. Liu Y, Gordesky-Gold B, Leney-Greene M, Weinbren NL, Tudor M, Cherry S. 2018. Inflammation-induced, STING-dependent autophagy restricts Zika virus infection in the *Drosophila* brain. Cell Host Microbe 24:57–68. https://doi.org/10.1016/j.chom.2018.05.022
15. Puig O, Marr MT, Ruhf ML, Tjian R. 2003. Control of cell number by *Drosophila* FOXO: downstream and feedback regulation of the insulin receptor pathway. Genes Dev 17:2006–2020. https://doi.org/10.1101/gad.1098703
16. Barbieri M, Bonafè M, Franceschi C, Paolisso G. 2003. Insulin/IGF-I-signaling pathway: an evolutionarily conserved mechanism of longevity from yeast to humans. Am J Physiol Endocrinol Metab 285:E1064–E1071. https://doi.org/10.1152/ajpendo.00296.2003
17. Šestan M, Marinović S, Kavazović I, Cekinović Đ, Wueest S, Turk Wensveen T, Brizić I, Jonjić S, Konrad D, Wensveen FM, Polić B. 2018. Virus-induced interferon-γ causes insulin resistance in skeletal muscle and derails glycemic control in obesity. Immunity 49:164–177. https://doi.org/10.1016/j.immuni.2018.05.005
18. del Campo JA, García-Valdecasas M, Rojas L, Rojas Á, Romero-Gómez M. 2012. The hepatitis C virus modulates insulin signaling pathway *in vitro* promoting insulin resistance. PLoS One 7:e47904. https://doi.org/10.1371/journal.pone.0047904
19. Yu B, Li C, Sun Y, Wang DW. 2021. Insulin treatment is associated with increased mortality in patients with COVID-19 and type 2 diabetes. Cell Metab 33:65–77. https://doi.org/10.1016/j.cmet.2020.11.014
20. Liang Q, Luo Z, Zeng J, Chen W, Foo S-S, Lee S-A, Ge J, Wang S, Goldman SA, Zlokovic BV, Zhao Z, Jung JU. 2016. Zika virus NS4A and NS4B proteins deregulate AKT-mTOR signaling in human fetal neural stem cells to inhibit neurogenesis and induce autophagy. Cell Stem Cell 19:663–671. https://doi.org/10.1016/j.stem.2016.07.019
21. Chan J-W, Zhu Z, Chu H, Yuan S, Chik K-H, Chan C-S, Poon V-M, Yip C-Y, Zhang X, Tsang J-L, Zou Z, Tee K-M, Shuai H, Lu G, Yuen K-Y. 2018. The celecoxib derivative kinase inhibitor AR-12 (OSU-03012) inhibits Zika virus via down-regulation of the Pi3K/AKT pathway and protects Zika virus-infected A129 mice: a host-targeting treatment strategy. Antiviral Res 160:38–47. https://doi.org/10.1016/j.antiviral.2018.10.007
22. Davenport AP, Hyndman KA, Dhaun N, Southan C, Kohan DE, Pollock JS, Pollock DM, Webb DJ, Maguire JJ. 2016. Endothelin. Pharmacol Rev 68:357–418. https://doi.org/10.1124/pr.115.011833
23. Correa AF, Bailão AM, Bastos IMD, Orme IM, Soares CMA, Kipnis A, Santana JM, Junqueira-Kipnis AP. 2014. The endothelin system has a significant role in the pathogenesis and progression of *Mycobacterium tuberculosis* infection. Infect Immun 82:5154–5165. https://doi.org/10.1128/IAI.02304-14
24. Notas G, Xidakis C, Valatas V, Kouroumalis A, Kouroumalis E. 2001. Levels of circulating endothelin-1 and nitrates/nitrites in patients with virus-related hepatocellular carcinoma. J Viral Hepat 8:63–69. https://doi.org/10.1046/j.1365-2893.2001.00269.x
25. Freeman BD, Machado FS, Tanowitz HB, Desruisseaux MS. 2014. Endothelin-1 and its role in the pathogenesis of infectious diseases. Life Sci 118:110–119. https://doi.org/10.1016/j.lfs.2014.04.021
26. Elisa T, Antonio P, Giuseppe P, Alessandro B, Giuseppe A, Federico C, Marzia D, Ruggero B, Giacomo M, Andrea O, Daniela R, Mariaelisa R, Claudio L. 2015. Endothelin receptors expressed by immune cells are involved in modulation of inflammation and in fibrosis: relevance to the pathogenesis of systemic sclerosis. J Immunol Res 2015:147616. https://doi.org/10.1155/2015/147616
27. George PM, Cunningham ME, Galloway-Phillipps N, Badiger R, Alazawi W, Foster GR, Mitchell JA. 2012. Endothelin-1 as a mediator and potential biomarker for interferon induced pulmonary toxicity. Pulm Circ 2:501–504. https://doi.org/10.4103/2045-8932.105039
28. Jiang ZY, Zhou QL, Chatterjee A, Feener EP, Myers MG, White MF, King GL. 1999. Endothelin-1 modulates insulin signaling through phosphatidylinositol 3-kinase pathway in vascular smooth muscle cells. Diabetes 48:1120–1130. https://doi.org/10.2337/diabetes.48.5.1120
29. Li Q, Park K, Li C, Rask-Madsen C, Mima A, Qi W, Mizutani K, Huang P, King GL. 2013. Induction of vascular insulin resistance and endothelin-1 expression and acceleration of atherosclerosis by the overexpression of protein kinase C-β isoform in the endothelium. Circ Res 113:418–427. https://doi.org/10.1161/CIRCRESAHA.113.301074
30. Hu Y, Flockhart I, Vinayagam A, Bergwitz C, Berger B, Perrimon N, Mohr SE. 2011. An integrative approach to ortholog prediction for disease-focused and other functional studies. BMC Bioinformatics 12:357. https://doi.org/10.1186/1471-2105-12-357
31. FlyBase gene report: Dmel\CG5326. 2023. https://flybase.org/reports/FBgn0038983.
32. FlyBase gene report: Dmel\TotF. 2023. https://flybase.org/reports/FBgn0044811.
33. FlyBase gene report: Dmel\CG43775. 2022. http://flybase.org/reports/FBgn0264297.
34. Purdy JG, Shenk T, Rabinowitz JD. 2015. Fatty acid elongase 7 catalyzes the lipidome remodeling essential for human cytomegalovirus replication. Cell Rep 10:1375–1385. https://doi.org/10.1016/j.celrep.2015.02.003
35. Ekengren S, Hultmark D. 2001. A family of turandot-related genes in the humoral stress response of *Drosophila*. Biochem Biophys Res Commun 284:998–1003. https://doi.org/10.1006/bbrc.2001.5067
36. Ferland DJ, Mullick AE, Watts SW. 2020. Chemerin as a driver of hypertension: a consideration. Am J Hypertens 33:975–986. https://doi.org/10.1093/ajh/hpaa084
37. Deng M, Yang S, Ji Y, Lu Y, Qiu M, Sheng Y, Sun W, Kong X. 2020. Overexpression of peptidase inhibitor 16 attenuates angiotensin II–induced cardiac fibrosis via regulating HDAC1 of cardiac fibroblasts. J Cell Mol Med 24:5249–5259. https://doi.org/10.1111/jcmm.15178
38. Regn M, Laggerbauer B, Jentzsch C, Ramanujam D, Ahles A, Sichler S, Calzada-Wack J, Koenen RR, Braun A, Nieswandt B, Engelhardt S. 2016. Peptidase inhibitor 16 is a membrane-tethered regulator of chemerin processing in the myocardium. J Mol Cell Cardiol 99:57–64. https://doi.org/10.1016/j.yjmcc.2016.08.010
39. Hope CM, Welch J, Mohandas A, Pederson S, Hill D, Gundsambuu B, Eastaff-Leung N, Grosse R, Bresatz S, Ang G, Papademetrios M, Zola H, Duhen T, Campbell D, Brown CY, Krumbiegel D, Sadlon T, Couper JJ, Barry SC. 2019. Peptidase inhibitor 16 identifies a human regulatory T-cell subset with reduced FOXP3 expression over the first year of recent onset type 1 diabetes. Eur J Immunol 49:1235–1250. https://doi.org/10.1002/eji.201948094
40. Ohno M, Sekiya T, Nomura N, Daito TJ, Shingai M, Kida H. 2020. Influenza virus infection affects insulin signaling, fatty acid-metabolizing enzyme expressions, and the tricarboxylic acid cycle in mice. Sci Rep 10:10879. https://doi.org/10.1038/s41598-020-67879-6
41. Xu J, Hopkins K, Sabin L, Yasunaga A, Subramanian H, Lamborn I, Gordesky-Gold B, Cherry S. 2013. ERK signaling couples nutrient status to antiviral defense in the insect gut. Proc Natl Acad Sci U S A 110:15025–15030. https://doi.org/10.1073/pnas.1303193110
42. DiAngelo JR, Bland ML, Bambina S, Cherry S, Birnbaum MJ. 2009. The immune response attenuates growth and nutrient storage in *Drosophila* by reducing insulin signaling. Proc Natl Acad Sci U S A 106:20853–20858. https://doi.org/10.1073/pnas.0906749106
43. Sansone CL, Cohen J, Yasunaga A, Xu J, Osborn G, Subramanian H, Gold B, Buchon N, Cherry S. 2015. Microbiota-dependent priming of antiviral intestinal immunity in *Drosophila*. Cell Host Microbe 18:571–581. https://doi.org/10.1016/j.chom.2015.10.010
44. Mi H, Muruganujan A, Ebert D, Huang X, Thomas PD. 2019. PANTHER version 14: more genomes, a new PANTHER GO-slim and improvements

in enrichment analysis tools. Nucleic Acids Res 47:D419–D426. https://doi.org/10.1093/nar/gky1038
45. Thomas PD, Ebert D, Muruganujan A, Mushayahama T, Albou L-P, Mi H. 2022. PANTHER: making genome-scale phylogenetics accessible to all. Protein Sci 31:8–22. https://doi.org/10.1002/pro.4218
46. Dagamajalu S, Rex DAB, Gopalakrishnan L, Karthikkeyan G, Gurtoo S, Modi PK, Mohanty V, Mujeeburahiman M, Soman S, Raju R, Tiwari V, Prasad TSK. 2021. A network map of endothelin mediated signaling pathway. J Cell Commun Signal 15:277–282. https://doi.org/10.1007/s12079-020-00581-4
47. Chahdi A, Sorokin A. 2008. Endothelin-1 couples βPix to p66Shc: role of βPix in cell proliferation through FOXO3a phosphorylation and p27kip1 down-regulation independently of AKT. Mol Biol Cell 19:2609–2619. https://doi.org/10.1091/mbc.e07-05-0424
48. Cifarelli V, Lee S, Kim DH, Zhang T, Kamagate A, Slusher S, Bertera S, Luppi P, Trucco M, Dong HH. 2012. FOXO1 mediates the autocrine effect of endothelin-1 on endothelial cell survival. Mol Endocrinol 26:1213–1224. https://doi.org/10.1210/me.2011-1276
49. Lu J-W, Liao C-Y, Yang W-Y, Lin Y-M, Jin S-L, Wang H-D, Yuh C-H, Gong Z. 2014. Overexpression of endothelin 1 triggers hepatocarcinogenesis in zebrafish and promotes cell proliferation and migration through the AKT pathway. PLoS One 9:e85318. https://doi.org/10.1371/journal.pone.0085318
50. Nihei S, Asaka J, Takahashi H, Kudo K. 2021. Bevacizumab increases endothelin-1 production via forkhead box protein O1 in human glomerular microvascular endothelial cells in vitro. Int J Nephrol 2021:8381115. https://doi.org/10.1155/2021/8381115
51. Renga B, Cipriani S, Carino A, Simonetti M, Zampella A, Fiorucci S. 2015. Reversal of endothelial dysfunction by GPBAR1 agonism in portal hypertension involves a AKT/FOXOA1 dependent regulation of H2S generation and endothelin-1. PLoS One 10:e0141082. https://doi.org/10.1371/journal.pone.0141082
52. Chen Q, Edvinsson L, Xu C-B. 2009. Role of ERK/MAPK in endothelin receptor signaling in human aortic smooth muscle cells. BMC Cell Biol 10:52. https://doi.org/10.1186/1471-2121-10-52
53. Foschi M, Chari S, Dunn MJ, Sorokin A. 1997. Biphasic activation of p21ras by endothelin - 1 sequentially activates the ERK cascade and phosphatidylinositol 3 - kinase. EMBO J 16:6439–6451. https://doi.org/10.1093/emboj/16.21.6439
54. Ersoy Y, Bayraktar NM, Mizrak B, Ozerol IH, Gunal S, Aladag M, Bayindir Y. 2006. The level of endothelin-1 and nitric oxide in patients with chronic viral hepatitis B and C and correlation with histopathological grading and staging. Hepatol Res 34:111–116. https://doi.org/10.1016/j.hepres.2005.11.005
55. Keller BC, Fredericksen BL, Samuel MA, Mock RE, Mason PW, Diamond MS, Gale M. 2006. Resistance to alpha/beta interferon is a determinant of West Nile virus replication fitness and virulence. J Virol 80:9424–9434. https://doi.org/10.1128/JVI.00768-06
56. Laurent-Rolle M, Boer EF, Lubick KJ, Wolfinbarger JB, Carmody AB, Rockx B, Liu W, Ashour J, Shupert WL, Holbrook MR, Barrett AD, Mason PW, Bloom ME, García-Sastre A, Khromykh AA, Best SM. 2010. The NS5 protein of the virulent West Nile virus NY99 strain is a potent antagonist of type I interferon-mediated JAK-STAT signaling. J Virol 84:3503–3515. https://doi.org/10.1128/JVI.01161-09
57. Lazear HM, Daniels BP, Pinto AK, Huang AC, Vick SC, Doyle SE, Gale M, Klein RS, Diamond MS. 2015. Interferon-λ restricts West Nile virus neuroinvasion by tightening the blood-brain barrier. Sci Transl Med 7:284ra59. https://doi.org/10.1126/scitranslmed.aaa4304
58. Lazear HM, Pinto AK, Vogt MR, Gale M, Diamond MS. 2011. Beta interferon controls West Nile virus infection and pathogenesis in mice. J Virol 85:7186–7194. https://doi.org/10.1128/JVI.00396-11
59. Samuel MA, Diamond MS. 2005. Alpha/beta interferon protects against lethal West Nile virus infection by restricting cellular tropism and enhancing neuronal survival. J Virol 79:13350–13361. https://doi.org/10.1128/JVI.79.21.13350-13361.2005
60. Diamond MS, Roberts TG, Edgil D, Lu B, Ernst J, Harris E. 2000. Modulation of Dengue virus infection in human cells by alpha, beta, and gamma interferons. J Virol 74:4957–4966. https://doi.org/10.1128/jvi.74.11.4957-4966.2000
61. Shives KD, Beatman EL, Chamanian M, O'Brien C, Hobson-Peters J, Beckham JD. 2014. West Nile virus-induced activation of mammalian target of rapamycin complex 1 supports viral growth and viral protein expression. J Virol 88:9458–9471. https://doi.org/10.1128/JVI.01323-14
62. Li Q, Zhang Y-Y, Chiu S, Hu Z, Lan K-H, Cha H, Sodroski C, Zhang F, Hsu C-S, Thomas E, Liang TJ, Luo G. 2014. Integrative functional genomics of hepatitis C virus infection identifies host dependencies in complete viral replication cycle. PLoS Pathog 10:e1004163. https://doi.org/10.1371/journal.ppat.1004163
63. Wang L, Yang L, Fikrig E, Wang P. 2017. An essential role of Pi3K in the control of West Nile virus infection. Sci Rep 7:3724. https://doi.org/10.1038/s41598-017-03912-5
64. Wang S, Xia P, Huang G, Zhu P, Liu J, Ye B, Du Y, Fan Z. 2016. FoxO1-mediated autophagy is required for NK cell development and innate immunity. Nat Commun 7:11023. https://doi.org/10.1038/ncomms11023
65. Daffis S, Lazear HM, Liu WJ, Audsley M, Engle M, Khromykh AA, Diamond MS. 2011. The naturally attenuated Kunjin strain of West Nile virus shows enhanced sensitivity to the host type I interferon response. J Virol 85:5664–5668. https://doi.org/10.1128/JVI.00232-11
66. Frias MA, Montessuit C. 2013. JAK-STAT signaling and myocardial glucose metabolism. JAKSTAT 2:e26458. https://doi.org/10.4161/jkst.26458
67. Gual P, Baron V, Lequoy V, Van Obberghen E. 1998. Interaction of Janus Kinases JAK-1 and JAK-2 with the insulin receptor and the insulin-like growth factor-1 receptor. Endocrinology 139:884–893. https://doi.org/10.1210/endo.139.3.5829
68. Hahn MB, Monaghan AJ, Hayden MH, Eisen RJ, Delorey MJ, Lindsey NP, Nasci RS, Fischer M. 2015. Meteorological conditions associated with increased incidence of West Nile virus disease in the United States, 2004-2012. Am J Trop Med Hyg 92:1013–1022. https://doi.org/10.4269/ajtmh.14-0737
69. Holcomb K. 2022. NOAA Climate.gov. Worst-ever U.S. West Nile virus outbreak potentially linked to a wetter-than-average 2021 Southwest monsoon
70. Saiz J-C. 2020. Animal and human vaccines against West Nile virus. Pathogens 9:1073. https://doi.org/10.3390/pathogens9121073
71. Elbadry MM, Tharwat M, Mohammad EF, Abdo EF. 2020. Diagnostic accuracy of serum endothelin-1 in patients with HCC on top of liver cirrhosis. Egypt Liver Journal 10:19. https://doi.org/10.1186/s43066-020-00030-2
72. Shi L, Zhou S-S, Chen W-B, Xu L. 2017. Functions of endothelin-1 in apoptosis and migration in hepatocellular carcinoma. Exp Ther Med 13:3116–3122. https://doi.org/10.3892/etm.2017.4314
73. Kalani M. 2008. The importance of endothelin-1 for microvascular dysfunction in diabetes. Vasc Health Risk Manag 4:1061–1068. https://doi.org/10.2147/vhrm.s3920
74. Lenoir O, Milon M, Virsolvy A, Hénique C, Schmitt A, Massé J-M, Kotelevtsev Y, Yanagisawa M, Webb DJ, Richard S, Tharaux P-L. 2014. Direct action of endothelin-1 on podocytes promotes diabetic glomerulosclerosis. J Am Soc Nephrol 25:1050–1062. https://doi.org/10.1681/ASN.2013020195
75. Shives KD, Massey AR, May NA, Morrison TE, Beckham JD. 2016. 4EBP-dependent signaling supports West Nile virus growth and protein expression. Viruses 8:287. https://doi.org/10.3390/v8100287
76. Harsh S, Ozakman Y, Kitchen SM, Paquin-Proulx D, Nixon DF, Eleftheriannos I. 2018. Dicer-2 regulates resistance and maintains homeostasis against Zika virus infection in *Drosophila* J Immunol 201:3058–3072. https://doi.org/10.4049/jimmunol.1800597
77. Jin Y-H, Kang B, Kang HS, Koh C-S, Kim BS. 2020. Endothelin-1 contributes to the development of virus-induced demyelinating disease. J Neuroinflammation 17:307. https://doi.org/10.1186/s12974-020-01986-z
78. Adams KL, Riparini G, Banerjee P, Breur M, Bugiani M, Gallo V. 2020. Endothelin-1 signaling maintains glial progenitor proliferation in the postnatal subventricular zone. Nat Commun 11:2138. https://doi.org/10.1038/s41467-020-16028-8
79. Koyama Y. 2013. Endothelin systems in the brain: involvement in pathophysiological responses of damaged nerve tissues. Biomol Concepts 4:335–347. https://doi.org/10.1515/bmc-2013-0004
80. Swire M, Kotelevtsev Y, Webb DJ, Lyons DA, Ffrench-Constant C. 2019. Endothelin signalling mediates experience-dependent myelination in the CNS. Elife 8:e49493. https://doi.org/10.7554/eLife.49493
81. Sejvar JJ. 2014. Clinical manifestations and outcomes of West Nile virus infection. Viruses 6:606–623. https://doi.org/10.3390/v6020606

82. Briese T, Jia XY, Huang C, Grady LJ, Lipkin WI. 1999. Identification of a Kunjin/West Nile-like flavivirus in brains of patients with New York encephalitis. Lancet 354:1261–1262. https://doi.org/10.1016/s0140-6736(99)04576-6
83. Perkins LA, Holderbaum L, Tao R, Hu Y, Sopko R, McCall K, Yang-Zhou D, Flockhart I, Binari R, Shim H-S, Miller A, Housden A, Foos M, Randkelv S, Kelley C, Namgyal P, Villalta C, Liu L-P, Jiang X, Huan-Huan Q, Wang X, Fujiyama A, Toyoda A, Ayers K, Blum A, Czech B, Neumuller R, Yan D, Cavallaro A, Hibbard K, Hall D, Cooley L, Hannon GJ, Lehmann R, Parks A, Mohr SE, Ueda R, Kondo S, Ni J-Q, Perrimon N. 2015. The transgenic RNAi project at Harvard medical school: resources and validation. Genetics 201:843–852. https://doi.org/10.1534/genetics.115.180208
84. Bellen HJ, Levis RW, He Y, Carlson JW, Evans-Holm M, Bae E, Kim J, Metaxakis A, Savakis C, Schulze KL, Hoskins RA, Spradling AC. 2011. The *Drosophila* gene disruption project: progress using transposons with distinctive site specificities. Genetics 188:731–743. https://doi.org/10.1534/genetics.111.126995
85. Ahlers LRH, Bastos RG, Hiroyasu A, Goodman AG. 2016. Invertebrate iridescent virus 6, a DNA virus, stimulates a mammalian innate immune response through RIG-I-like receptors. PLoS One 11:e0166088. https://doi.org/10.1371/journal.pone.0166088
86. Zhang W, Thompson BJ, Hietakangas V, Cohen SM, Rulifson E. 2011. MAPK/ERK signaling regulates insulin sensitivity to control glucose metabolism in *Drosophila*. PLoS Genet 7:e1002429. https://doi.org/10.1371/journal.pgen.1002429
87. Goodman AG, Fornek JL, Medigeshi GR, Perrone LA, Peng X, Dyer MD, Proll SC, Knoblaugh SE, Carter VS, Korth MJ, Nelson JA, Tumpey TM, Katze MG. 2009. "P58(IPK): a novel "CIHD" member of the host innate defense response against pathogenic virus infection". PLoS Pathog 5:e1000438. https://doi.org/10.1371/journal.ppat.1000438
88. Subramanian A, Tamayo P, Mootha VK, Mukherjee S, Ebert BL, Gillette MA, Paulovich A, Pomeroy SL, Golub TR, Lander ES, Mesirov JP. 2005. Gene set enrichment analysis: a knowledge-based approach for interpreting genome-wide expression profiles. Proc Natl Acad Sci U S A 102:15545–15550. https://doi.org/10.1073/pnas.0506580102
89. Palu RAS, Ong E, Stevens K, Chung S, Owings KG, Goodman AG, Chow CY. 2019. Natural genetic variation screen in *Drosophila* identifies Wnt signaling. G3 GenesGenomesGenetics 9:3995–4005. https://doi.org/10.1534/g3.119.400722
90. Martin M, Hiroyasu A, Guzman RM, Roberts SA, Goodman AG. 2018. Analysis of *Drosophila* STING reveals an evolutionarily conserved antimicrobial function. Cell Rep 23:3537–3550. https://doi.org/10.1016/j.celrep.2018.05.029
91. Spellberg MJ, Marr MT. 2015. FOXO regulates RNA interference in *Drosophila* and protects from RNA virus infection. Proc Natl Acad Sci U S A 112:14587–14592. https://doi.org/10.1073/pnas.1517124112
92. Torres MJ, López-Moncada F, Herrera D, Indo S, Lefian A, Llanos P, Tapia J, Castellón EA, Contreras HR. 2021. Endothelin-1 induces changes in the expression levels of steroidogenic enzymes and increases androgen receptor and testosterone production in the PC3 prostate cancer cell line. Oncol Rep 46:171. https://doi.org/10.3892/or.2021.8122